Fiber Transmission for Sub-500-fs Pulses Using a Dispersion-Compensating Fiber

Cheng-Chun Chang and Andrew M. Weiner, *Fellow, IEEE*

***Abstract*— We report transmission of ∼60-fs and ∼245-fs pulses, respectively, over 42-m and 2.5-km fiber links which consist of standard single-mode fibers (SMF) concatenated with dispersion-compensating fibers (DCF). The experiments using very short pulses (∼60 fs) over a short fiber length (∼42 m) demonstrate the ability to achieve simultaneous dispersion and dispersion slope compensation using this technique. Femtosecond spectral interferometry measurements of this 42-m link show that its residual dispersion slope is approximately six times lower than that of the dispersion-shifted fiber. Finally, to demonstrate that the dispersion-limited propagation distance is proportional to the cube of the pulsewidth, we transmit ∼245-fs pulses over a 2.5-km SMF–DCF link and achieve comparable pulse restoration as with the shorter fiber experiments.**

***Index Terms*— Dispersion compensation, dispersion measurement, spectral interferometry.**

I. Introduction

WITH FIBER loss being compensated by fiber amplifiers, fiber group-velocity dispersion (GVD) has become a major factor in limiting short-pulse transmission. Dispersion and dispersion compensation are then key issues for high-speed lightwave transmission systems, especially time-division multiplexed (TDM) [1] and code-division multiple-access (CDMA) systems [2]. A variety of dispersion compensation techniques have been investigated, mostly for the purpose of upgrading embedded standard single-mode fibers (SMF's) with a large anomalous dispersion $(D = 17$ ps/km/nm at 1.55 μm$)$, for use in state-of-the-art 1.55-μm systems experiments operating at ∼10 Gb/s and above. These include techniques utilizing chirped fiber Bragg gratings [3]–[6], bulk grating-and-lens pairs [7], mid-span spectral inversion [8]–[11], and dispersion-compensating fibers [12]–[15]. In addition, a number of fiber experiments exploring linear dispersion compensation with ultrashort (femtosecond) pulses are now beginning to appear. For pulses in the femtosecond regime, simultaneous compensation of both second- and third-order dispersion (or dispersion and dispersion slope) is necessary [7], [16]. One recent system experiment used linear propagation with dispersion and partial-dispersion slope compensation for transmission of 980-fs pulses over 40 km of fiber to demonstrate 400-Gb/s TDM transmission [17]. Linearly chirped fiber Bragg gratings have been used to compensate the second-order but not the third-order dispersion for ∼500-fs pulses transmitted over 245 m of SMF [3] and 3.9 km of dispersion-shifted fiber (DSF) [4]. Recently, continously chirped fiber gratings with a high reflectivity bandwidth of ∼5.2 nm have been used for dispersion compensation in 40-Gb/s system experiments using SMF; however, phase variations within the high reflectivity bandwidth still appear to limit these devices to picosecond applications [6]. Transmission of 150- and 500-fs pulses was demonstrated, respectively, over 400 m and 3.2 km of DSF using a bulk grating-and-lens apparatus [7], which can simultaneously compensate both second- and third-order dispersion when operating at wavelengths shorter than the fiber zero dispersion wavelength (λ_0). Here we apply the dispersion-compensating fiber approach to achieve simultaneous dispersion and dispersion slope compensation for transmission of ultrashort (62 and 245 fs) pulses over ∼40-m and ∼2.5-km fiber links respectively, in an all-fiber system. We note that for femtosecond pulses, dispersion-compensated linear pulse propagation may lead to longer transmission distances than possible with solitons, which are limited in the femtosecond regime by higher order effects like the Raman self-frequency shift [18].

The idea of using a special dispersion-compensating fiber (DCF) to compensate the dispersion in SMF was proposed as early as 1980 [19]. Early dispersion compensation experiments [12]–[14] used relatively long pulses $(\geq$10 ps) and DCF with negative (or normal) dispersion (opposite of SMF) but positive dispersion slope (same as SMF) in the 1550-nm wavelength range. Consequently, although the second-order dispersion of the composite fiber link was compensated, the third-order dispersion was increased. Such DCF's are not desirable for femtosecond pulse propagation. In our experiments, we are interested in extending the DCF technique to achieve simultaneous second- and third-order dispersion compensation for femtosecond pulses. The possibility of simultaneous dispersion and dispersion slope compensation were first demonstrated using higher order fiber modes to enable broad-band dispersion compensation for several WDM channels [15]. Here we employ a single-mode DCF which exhibits both negative dispersion and *negative* dispersion slope [20] for femtosecond-pulse dispersion compensation. We first tested this DCF by demonstrating nearly dispersionless transmission of 62-fs pulses over a 42-m concatenated fiber link consisting of standard SMF and DCF [21]. To evaluate the performance limits of this technique, we utilized femtosecond spectral interferometry for *in situ* characterization of the small residual dispersion of this 42-m dispersion-compensated SMF–DCF

Manuscript received February 10, 1997; revised May 16, 1997. This work was supported by the National Science Foundation under Grant ECS-9 312 256 and Grant ECS-9 626 967.

The authors are with the School of Electrical and Computer Engineering, Purdue University, West Lafayette, IN 47907 USA.

Publisher Item Identifier S 0018-9197(97)06219-2.

fiber link. As we will show later, the residual dispersion of such dispersion-optimized link is dominated by third-order dispersion (dispersion slope) with a value six times lower than that of DSF. To our knowledge, this is the first time that spectral interferometry has been used for measuring a fiber as long as tens of meters. Our experiments transmitting very short sub-100-fs pulses over a short distance (42 m) serve as an extremely sensitive test of the broad-band dispersion compensation capabilities of such links and allow us to predict the performance of experiments using longer (a few hundred femtoseconds) pulses and substantially longer links. To demonstrate this point, we have transmitted longer, ~245-fs input pulses over a 2.5-km length of a similar SMF–DCF combination. Our results confirm the expectation [21] that the propagation distance should scale with pulsewidth to the third power. We also note that our demonstration of several kilometer propagation of several hundred femtosecond pulses should enable tests of novel code-division multiple-access local-area networking schemes [2].

This paper is structured as follows. We briefly review the dispersion compensation technique using DCF in Section II. In Section III, we describe our experimental apparatus and describe the results of the 42-m fiber transmission experiments. In Section IV, we discuss the femtosecond spectral interferometry technique and report its application for measurements of the 42-m fiber. The 2.5-km fiber transmission experiments for 245-fs pulses are described in Section V. In Section VI, we summarize.

II. Dispersion Compensation Using DCF

The effects of GVD can be accounted for by expanding the group delay $T(\omega)$ per unit length, defined as $d\beta/d\omega$ (inverse of group velocity) about the center frequency ω_c as

$$T(\omega)=\frac{1}{v_g}=\frac{d\beta(\omega)}{d\omega}=\beta_1+\beta_2(\omega-\omega_c)+\frac{\beta_3}{2}(\omega-\omega_c)^2+\cdots \quad (1)$$

where

$$\beta_m=\left[\frac{d^m\beta}{d\omega^m}\right]_{\omega=\omega_c},\qquad m=0,1,2,3,\cdots. \quad (2)$$

β_1 is the group delay for the center frequency ω_c, the time required for the center frequency component to travel unit distance. β_m is called the mth order dispersion. As frequency moves away from ω_c, the group delay deviates from β_1 on account of all orders of dispersion. Also, as pulses get shorter, the group delay spread increases because the spectral spread $(\omega-\omega_c)$ increases. Therefore, the dispersion effects increase as the pulsewidth decreases. Dispersion effects are also often expressed in terms of the variation in the group delay with respect to deviations in *wavelength* as follows:

$$D(\lambda)=\frac{dT(\omega)}{d\lambda}=\frac{d}{d\lambda}\left(\frac{d\beta}{d\omega}\right)=D(\lambda_c)+D'(\lambda_c)(\lambda-\lambda_c)+\cdots. \quad (3)$$

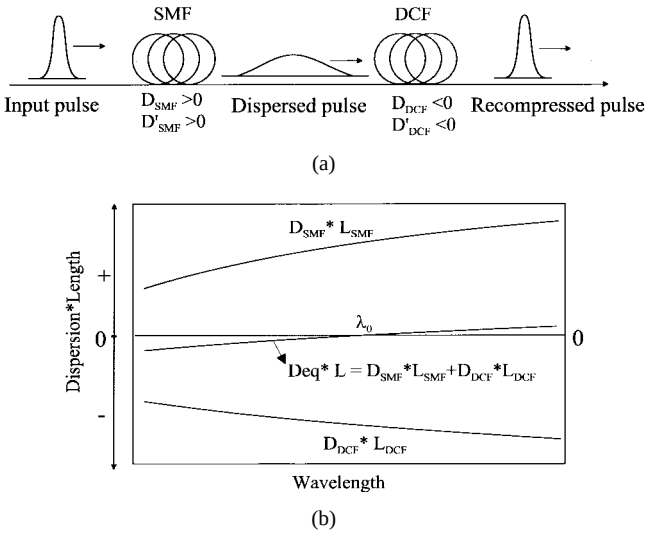

Fig. 1. Schematics of dispersion compensation using DCF. (a) Schematic of a concatenated SMF–DCF link. (b) Schematic dispersion curves of a SMF, a DCF, and a concatenated SMF–DCF link.

Here $'$ means derivative with respect to wavelength λ. $D(\lambda_c)$ and $D'(\lambda_c)$ are called dispersion and dispersion slope, respectively (sometimes referred to as second- and third-order dispersion as well). β_2 and β_3 are closely related to D and D' as

$$D=-(2\pi c/\lambda^2)\beta_2 \quad (4)$$

$$D'=(2\pi c/\lambda^2)^2\beta_3+(4\pi c/\lambda^3)\beta_2. \quad (5)$$

$\beta_2>0\quad(D<0)$ is called normal dispersion, while $\beta_2<0\,(D>0)$ is denoted anomalous dispersion. In the normal-dispersion regime, the higher frequency components of a pulse travel more slowly than the lower frequency components. The opposite occurs in the case of anomalous dispersion. Both kinds of dispersion broaden the pulses and introduce a frequency chirp (approximately linear when the second-order dispersion dominates).

The scheme using DCF's is a linear, all-fiber technique which is very simple in concept and in implementation [12]–[15]. The idea of this technique is to concatenate a SMF with a DCF whose dispersion is equal in magnitude and opposite in sign to that of the SMF. As a result, the pulses broadened by SMF were recompressed by the DCF, as schematically illustrated in Fig. 1(a). The concatenated SMF–DCF fiber link can be characterized by an equivalent dispersion $D_{\rm eq}$ which is equal to the overall dispersion averaged over the total length of the fiber link. The equivalent dispersion is given by

$$D_{\rm eq}(\lambda)=[R*D_{\rm SMF}(\lambda)+D_{\rm DCF}(\lambda)]/(1+R) \quad (6)$$

where R is the length ratio of the SMF to DCF, $D_{\rm SMF}$ is the dispersion of the SMF and $D_{\rm DCF}$ is the dispersion of the compensating fiber. Since the conventional SMF has a positive (anomalous) dispersion $D(\lambda)$ and a positive dispersion slope $D(\lambda)'$ at 1550-nm wavelength range, a favorable DCF should be a single-mode fiber with a large negative (normal) dispersion and a negative dispersion slope. Such a

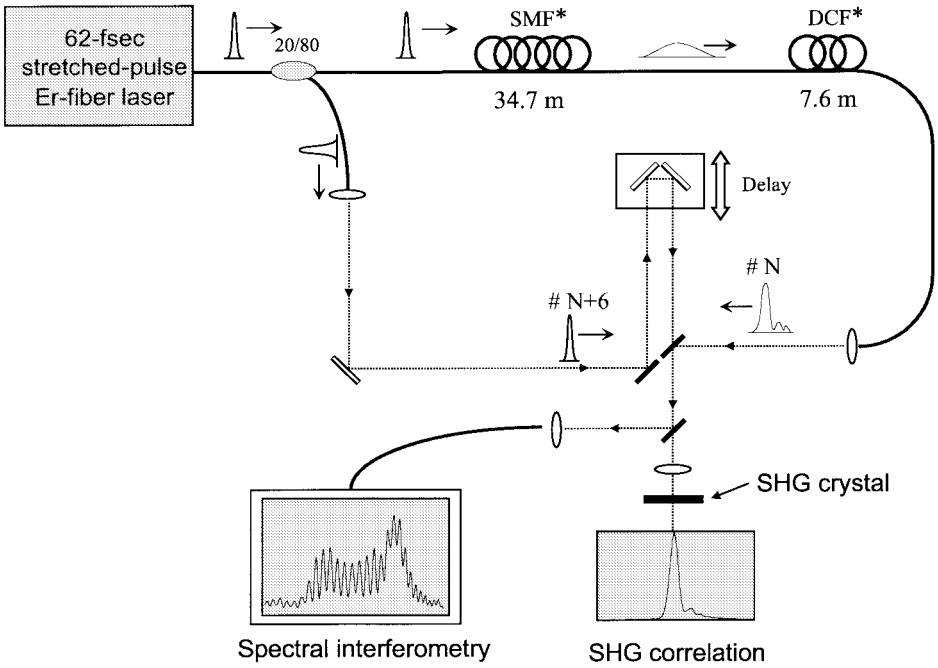

Fig. 2. The experimental layout for dispersion compensation experiments. 20/80: 20/80 fiber coupler; SMF: standard single-mode fiber; DCF: dispersion compensating fiber; SHG: second harmonic generation. The setup for SHG correlation measurements can be easily modified for spectral interferometry measurements by inserting a mirror in front of a SHG crystal.

DCF can be achieved by the proper design of the refractive-index profile [20]. When concatenated with a SMF, such a DCF not only eliminates dispersion at certain wavelengths but also significantly reduces the overall dispersion slope, as illustrated schematically in Fig. 1(b). Complete elimination of the second- and third-order dispersion simultaneously requires DCF that satisfies the following relation:

$$\left(\frac{D'(\lambda_c)}{D(\lambda_c)}\right)_{\mathrm{DCF}} = \left(\frac{D'(\lambda_c)}{D(\lambda_c)}\right)_{\mathrm{SMF}}. \tag{7}$$

In practice, it is difficult to make such a perfectly matched DCF. However the combination of two DCF's, one with D'/D larger than SMF and the other with smaller D'/D, should be capable of completely compensating the dispersion and dispersion slope for a wide wavelength range since both DCF lengths can be adjusted, providing one more degree of freedom to adjust the overall dispersion.

III. 42-m Dispersion-Compensated SMF–DCF Link

For our first experiment, we characterize the propagation of sub-100-fs pulses over a short distance (~42 m) SMF–DCF link [21]. As illustrated in Fig. 2, femtosecond pulses from a mode-locked fiber laser are split into two by a 20/80 fiber coupler. Eighty percent of the power is sent to a concatenated SMF–DCF fiber link. The output pulses from the fiber link are measured by performing noncollinear second harmonic generation (SHG) intensity cross-correlation measurements using short (unbroadened) reference pulses which emerge out of the 20% port of the fiber coupler. The reference pulses and the output pulses from the fiber link could also be combined for spectral interferometry measurements, detailed in Section IV.

The femtosecond pulse source for our experiments was a stretched-pulse mode-locked Er-doped fiber ring laser [22]. The detail of this fiber laser is described in [21]. Our laser generates a stable train of femtosecond pulses at a 34-MHz repetition rate, with one pulse per cavity round-trip time. Fig. 3(a) shows the power spectrum and Fig. 3(b) the intensity autocorrelation of the mode-locked pulses. The power spectrum has a full-width at half-maximum (FWHM) bandwidth of ~60 nm and exhibits several interesting features: sharp peaks at 1560 nm and 1610 nm, as well as clear sidelobes at 1510 and 1645 nm. These features may be evidence of optical wave-breaking [23] occurring within our laser cavity. The autocorrelation width of 95-fs FWHM as indicated in Fig. 3(b) corresponds to an intensity pulse width of 62-fs FWHM, assuming a secant hyperbolic pulse shape.

Our link is composed of ~34.7 m of AT&T 5D single-mode fiber and ~7.6 m of DCF (AT&T JRFDC1074C1DC). The SMF has $D \approx 17$ ps/km/nm (or $\beta_2 \approx -22$ ps^2/km) and $D' \approx 0.05$–0.06 ps/km/nm^2 at 1550 nm. The DCF has $D \approx -76$ ps/km/nm measured by time-of-flight technique and a negative dispersion slope $D' \approx 0.2$ ps/km/nm^2. To optimize the overall link dispersion, we iteratively adjusted and fine-tuned the lengths of SMF and DCF in order to reduce the duration of the output signal pulse to the shortest possible. The cross-correlation trace of the shortest output pulses is shown in Fig. 4(a). The correlation width is 125-fs FWHM, corresponding to a deconvolved pulse duration of ~110 fs, which is within a factor of two of the reference pulse duration. The 62-fs pulses would be broadened to ~35 ps (calculated) after traveling through the SMF section alone; but by virtue of the DCF the final output pulse is recompressed to ~110 fs, resulting in a compression ratio of ~300. To our knowledge, this is the first experimental demonstration

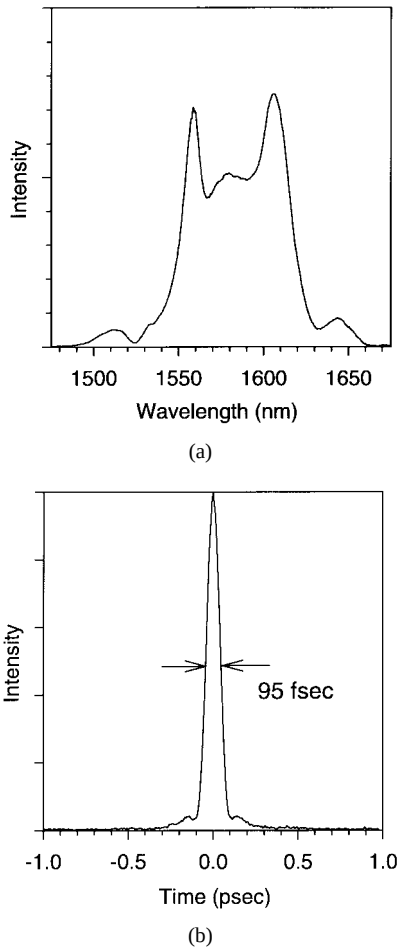

Fig. 3. Femtosecond pulses from a stretched-pulse mode-locked fiber ring laser. (a) Power spectrum. (b) Background-free autocorrelation. The 95-fs autocorrelation width corresponds to a deconvolved pulsewidth of ~62 fs.

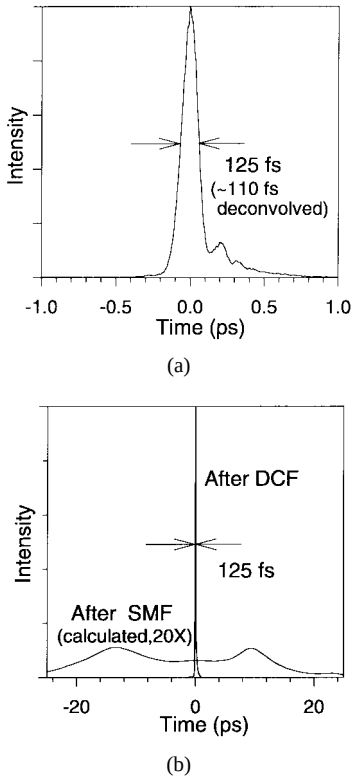

Fig. 4. (a) Intensity profile of the output pulse from the optimally dispersion-compensated fiber link, measured by cross correlation using a reference pulse directly from the laser. The 125-fs cross-correlation width corresponds to a deconvolved pulsewidth of ~110 fs. (b) The output pulse from Fig. 3(a) superimposed on the calculated pulse after propagation through 35-m of SMF alone (magnified by 20 times). This dispersion-compensated pulse shows a recompression ratio of 300.

of sub-100-fs pulse propagation over several tens of meters of fiber. In order to illustrate the magnitude of pulse stretching and successful recompression, Fig. 4(b) shows the trace of the optimally recompressed signal pulse together with the calculated broadened 35-ps pulse (the intensity of the 35-ps pulse is magnified 20 times in order to be discernible). The shortest output pulses are obtained for an optimal fiber length ratio $R_{\rm opt} \sim 4.57$ (34.7 m/7.6 m). The pulse duration increases by 10% when the length ratio is changed by ~0.15%. This indicates that accurate adjustment of the length ratio is important for the success of the DCF technique, as expected for our case of very high recompression ratio.

As shown in Fig. 4(a), there is a small oscillation in the trailing tail of the output pulse, a phenomenon typical of positive third-order dispersion. This means that the second-order dispersion of the fiber link is almost completely compensated and the residual dispersion is dominated by third-order dispersion. To quantitatively characterize the performance of the DCF, the magnitude of this residual third-order dispersion and the zero-dispersion wavelength should be measured. However, since intensity cross-correlation measurements do not provide any phase information and since the laser power spectrum is of an irregular shape, it's difficult to make accurate estimates for the residual dispersion and zero dispersion wavelength from the intensity profile of the output pulse alone. In the next section, we will present a spectral interferometry technique which is capable of measuring both phase and amplitude in order to characterize the residual dispersion of the fiber link.

IV. Fiber Dispersion Measurements Using Spectral Interferometry

Fiber dispersion can be measured by a number of measurement techniques, as reviewed in [24] and [25]. These include time-of-flight measurements and related frequency-domain phase-shift measurements, as well various interferometric measurements. The time-of-flight and related techniques generally require a minimum of 1 km of fiber in order to obtain reasonable precision with sufficient wavelength resolution. The interferometric techniques, either time-domain interferometry or spectral interferometry, are usually performed with very short fiber lengths on the order of 1 m. This limitation stems from the need for a free-space reference arm with a delay equal to that experienced in the fiber. Here we demonstrate the use of spectral interferometry to characterize the 42-m dispersion-compensated SMF–DCF fiber link. To our knowledge, this is the first time that spectral interferometry has been used for measuring a fiber as long as tens of meters. Our experiments using extremely short pulses (<100 fs) serve as an extremely sensitive test for measuring small amounts of residual dispersion in the compensated fiber link. The results of our measurements can be used to extrapolate dispersion compensation performance for somewhat longer pulses (a few

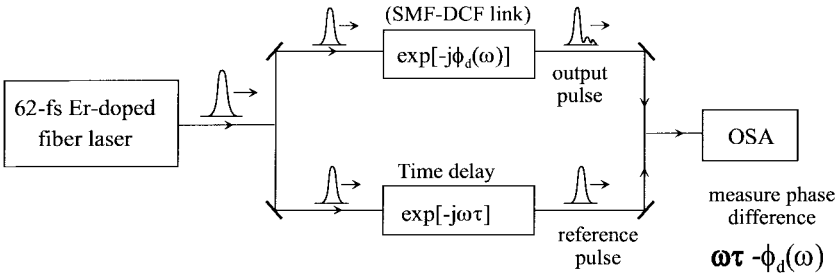

Fig. 5. Schematic of spectral interferometry. Pulses from a mode-locked erbium fiber laser are sent to a Mach–Zender interferometer. The coherent superposition of the distorted pulse and the time-delayed but undistorted pulse are recorded by an OSA.

hundred femtoseconds) over fiber links in the kilometer range suitable for local-area network applications.

Spectral interferometry measurements can be performed using either incoherent or ultrashort pulse light sources. Incoherent white light sources have been applied principally for characterization of short ($\sim$1 m) single-mode fibers [26], [27]. Coherent ultrashort pulse sources have been applied, for example, to measure self-phase-modulation [28] and polarization-mode dispersion [29]. Spectral interferometry measurements using ultrashort optical pulses have also become popular for measurement of various bulk optical systems used in ultrafast optics applications [30]. Here we apply ultrabroadband ($>$50 nm) femtosecond pulses from our mode-locked fiber laser for fiber dispersion measurements. The periodic nature of the mode-locked laser output allows us to correlate the pulses emerging from the fiber under test with pulses emitted substantially later from the laser. This eliminates the need for a long free-space reference arm and therefore leads to the ability to perform spectral interferometry measurements with much longer fibers. Our measurements reveal that the concatenated SMF–DCF fiber link has approximately zero second-order dispersion and a reduced third-order dispersion (dispersion slope) roughly six times smaller than that of dispersion-shifted fiber.

Fig. 5 shows the schematic of our femtosecond spectral interferometry measurements. As before, 62-fs pulses from the stretched-pulse mode-locked Er-doped fiber ring laser were split into the two arms of a Mach–Zender interferometer. One arm of the interferometer is a free-space reference arm whose length can be varied using a stepper motor driven translation stage to introduce a time delay τ. The other (signal arm) contains the optical system to be measured, which in our case is the 42-m dispersion-compensated SMF–DCF fiber link. If there are no nonlinear effects, the power spectrum $S(\omega)$ recorded by the optical spectrum analyzer at the output of the interferometer can be expressed as

$$\begin{aligned} S(\omega) &= |E(\omega)e^{-j\omega\tau} + aE(\omega)e^{-j\phi_d(\omega)}|^2 \\ &= |E(\omega)|^2\{1 + a^2 + 2a\cos[\omega\tau - \phi_d(\omega)]\} \end{aligned} \quad (8)$$

where $E(\omega)$ is the spectrum of the 62-fs input pulse and a^2 is the power split ratio of the two arms. The argument of the cosine term in the above equation is the phase difference of the two arms (denoted as $\phi(\omega)$) which contains the linear phase shift $\omega\tau$ due to fixed time delay τ as well as the phase distortion $\phi_d(\omega)$ due to fiber dispersion. The optical path length of the reference arm is adjusted to equal that of the signal arm containing the fiber within a small adjustable delay τ, modulo the 30-ns pulse repetition period of the laser pulses. In our experiments, signal pulses passing through the fiber correlate with the sixth successive pulse passing through the reference arm. This periodic correlation property of the mode-locked laser circumvents the need for very long free-space delay arms and thus enables spectral interferometry to be applied to fibers more than an order of magnitude longer than previously. The setup used for intensity cross-correlation measurements in our dispersion compensation experiments in the previous section can be easily modified for spectral interferometry measurements. As illustrated in Fig. 2, both the signal and the reference beams are redirected by inserting a moving mirror in front of the SHG crystal and then coupled into a single-mode fiber patchcord connected to an optical spectrum analyzer (OSA) which records the spectrum of the superimposed pulses. Although the two beams are in a noncollinear configuration, the core of the single-mode fiber patchcord samples a spot smaller than a single spatial fringe and therefore maintains a high-contrast spectral interference pattern. The biggest concern in our experiments is the need to ensure that the interferometer path difference does not drift during the course of a measurement. In order to protect against such drift, we set the OSA for rapid scans, typically $\sim$1–2-s scan times over a 120-nm range, with a spectral resolution of 0.1 nm. We also checked for consistency by repeating each fiber measurement roughly ten times with various values of the delay τ.

For both dispersion compensation and spectral interferometry measurements, the average optical power sent to the concatenated fiber link is typically $\sim$1 mW, corresponding to a peak power of $\sim$425 W ($\sim$4.5% of the $N = 1$ soliton power for 62-fs pulses in SMF) at the input of to the fiber link. Because the pulsewidth broadens rapidly in the first few meters of propagation, accumulated nonlinear phase shifts are expected to be very small. This contention is supported by nonlinear Schrödinger equation simulations reported elsewhere [31]. The power spectrum measured from the output of the 42-m link appears similar to the input spectrum for average powers up to $\sim$3 mW, the highest we have available, providing further evidence that we are operating in the linear transmission regime as desired.

Two examples of spectral interferograms were obtained for time delays of -2.9 ps (reference pulse ahead) and $+1.7$ ps, respectively. Noise in the interferograms is suppressed by lowpass filtering (in the time domain); the results are shown in Fig. 6(a) and (b). The periodicity of the spectral fringes in

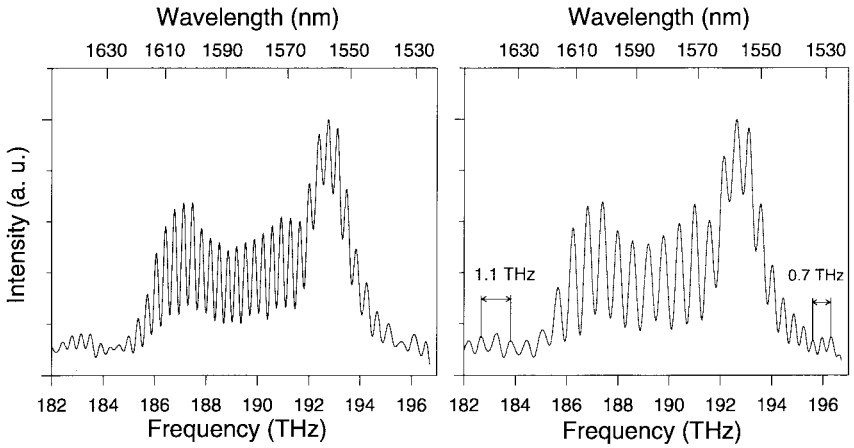

Fig. 6. Spectral interference patterns. The filtered version of the interferograms recorded by the OSA corresponding to time delay of (a) -2.9 ps (reference pulse ahead) and (b) $+1.7$ ps. Small variations in the periodicity of the intensity peaks across the spectrum are caused by the residual dispersion of the 42-m fiber link.

Fig. 6 should be inversely proportional to the constant time delay τ, as illustrated by the obviously different periodicities in Fig. 6(a) and (b) which correspond to different time delays. Also note that the periodicity is not constant but varies slowly with frequency. These variations in periodicity arise from the phase distortions caused by the fiber dispersion; this is the information we would like to extract from the interferograms. These filtered interferograms are subsequently normalized by the spectrum of the input pulse, $|E(\omega)|^2$, in order to isolate the dc and the cosine terms in (8). We then obtain the spectral phase $\phi(\omega)$ by locating the position of the maxima in the normalized filtered data and assigning a 2π phase shift between adjacent spectral peaks. The resultant phase versus frequency data are fit to the following equation:

$$\phi(\omega) = \omega\tau - \phi_d(\omega) = b_0 + \tau(\omega - \omega_c) - \frac{\beta_2}{2}L(\omega - \omega_c)^2 - \frac{\beta_3}{6}L(\omega - \omega_c)^3 - \cdots \quad (9)$$

where β_n is called the nth-order dispersion and L is the length of the fiber link. The linear phase term due to the fixed time delay, $\omega\tau$, is then subtracted to yield only the phase distortion $\phi_d(\omega)$ due to dispersion. Curves A and B in Fig. 7 show the resulting phase shifts corresponding to $\phi_d(\omega)$ evaluated at the positions of the spectral peaks in the data sets of Fig. 6. The solid lines are the least-square fits of each data set to third-order polynomials. From these data, as well as from several other measurements performed at different delays τ, the residual dispersion in the concatenated link is dominated by third-order dispersion with $\beta_3 \sim 0.016 \pm 0.002$ ps^3/km ($D' \sim 0.0088 \pm 0.001$ ps/km/nm^2) (which means $\sim$85% of the dispersion slope of the SMF has been compensated) and with zero dispersion wavelength ($\beta_2 = 0$) at 1591 ± 3 nm. This result is consistent with the intensity cross-correlation measurement shown in Fig. 4(a) which displays an oscillatory trailing tail arising from this third-order dispersion. The measured third-order dispersion is roughly six times lower than that of dispersion-shifted fiber, where $D' \sim 0.05$–0.06 ps/km/nm^2.

In order to further validate this spectral interferometry technique, we have also measured some short fibers with known dispersions. Curves C, D, and E in Fig. 7 show the measured results for three additional fiber configurations: 1-m DSF spliced to 20-cm SMF, 1-m DSF spliced to 30-cm SMF, and 1-m DSF spliced to 10-cm DCF. The dispersion of SMF can be obtained from these measurements by taking the phase difference of curves C and D, which corresponds to the phase distortion caused by 10 cm of SMF. Similarly, the dispersion of the DCF can then be deduced from the difference of curves C and E after the dispersion of SMF has been obtained. Our measurements yield $\beta_2 \sim -21.0 \pm 1.5$ ($D \sim 16.5$ ps/km/nm) and 98.5 ± 7.5 ps^2/km ($D \sim 77.3$ ps/km/nm) at 1550 nm for SMF and DCF, respectively. Compared to the known second-order dispersions of SMF ($\beta_2 = -22$ ps^2/km) and of this DCF ($\beta_2 = 96$ ps^2/km) at 1550 nm (obtained from the time-of-flight measurements), these results indicate that our spectral interferometry measurements yield accurate values for β_2, the leading-order dispersion term in these three fiber configurations. Therefore, we believe that the measured residual dispersion β_3 for the dispersion-compensated SMF–DCF link should also be valid, because third-order dispersion is the leading-order dispersion term for this compensated fiber link. Note that we directly measured the overall dispersion of the whole SMF–DCF fiber link, rather than measuring the dispersion of the individual fibers separately and weighting them according to their lengths, because we are only interested in the overall uncompensated dispersion effect. Furthermore, measuring the whole link directly provides the most accurate estimate of the total link dispersion (which is dominated by third-order dispersion β_3), while in the individual SMF or DCF the β_2 is dominant.

Spectral interferometry measurements can potentially be extended to longer fibers, limited ultimately by laser timing jitter. In the current experiments, the timing jitter between pulses number N and $N + 6$ is required to be less than roughly 1 fs to avoid washing out the spectral fringes. Recent measurements in a stretched-pulse mode-locked fiber laser similar to ours showed a white noise timing jitter ranging from 4 to 19 ppm with a 10-Hz resolution bandwidth, depending on the laser configuration [32]. Scaling these numbers to our experiments would lead to a timing jitter between pulses N and

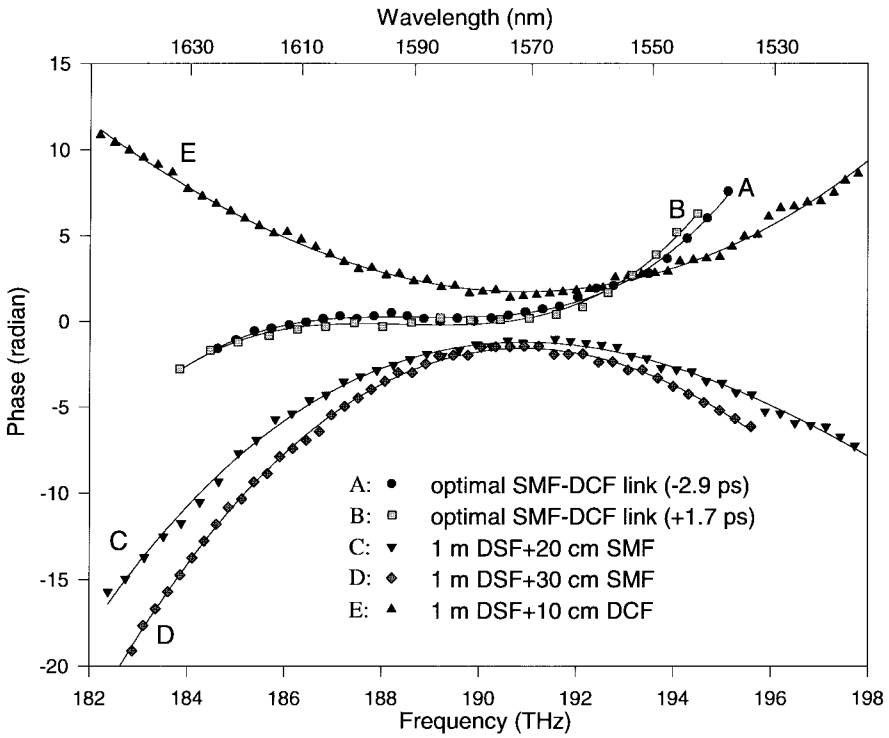

Fig. 7. Spectral phase shifts for interferograms. Curves A and B showing the phase distortion $\phi_d(\omega)$ of the optimally dispersion-compensated link are derived from the interferograms in Fig. 3, respectively. Curves C, D, and E correspond to the phase distortion $\phi_d(\omega)$ of three fiber configurations, respectively, 1-m DSF + 20-cm SMF, 1-m DSF + 30-cm SMF, and 1-m DSF + 10-cm DCF.

$N+6$ in the range 0.16–0.76 fs, consistent with our observation of high-contrast spectral fringes. Based on the more favorable (lower) jitter estimate of 4 ppm, one could in principle apply spectral interferometry to fibers over one kilometer in length. Furthermore, note that mode-locked semiconductor laser systems can have timing jitters approximately ten times lower over the same resolution bandwidth [33], which could further extend the maximum fiber length. These estimates, which do not account for correlated noise effects such as long-term drift of the laser repetition rate or the optical length of the fiber under test, should be regarded as upper limits to the permissible fiber length. We note that spectral interferometry can also be performed on a single-shot (single-pulse) basis, in which case the limitations outlined above do not apply.

To summarize for this section, we demonstrate the application of femtosecond spectral interferometry to measure the small residual third-order dispersion of a 42-m dispersion-compensated fiber link. By using a mode-locked pulsed source, we were able to extend our spectral interferometric measurement technique substantially beyond the usual fiber lengths on the order of a meter. It should be possible to extend interferometric techniques to even longer fibers as well, limited ultimately by laser timing jitter.

V. 2.5-km Dispersion-Compensated SMF–DCF Link

Substantially longer transmission distances should be possible with longer femtosecond pulses if the dispersion characteristics we have measured for the 42-m link can be scaled to longer concatenated SMF–DCF links. For a fiber link dominated by third-order dispersion, the propagation distance is proportional to the third power of pulsewidth for a fixed pulse broadening ratio [34]. Therefore, from the case of 62-fs pulses traveling over a 42-m SMF–DCF fiber link, we should expect a comparable pulse-broadening ratio for 245-fs pulses to propagate over a similar SMF–DCF link of 2.6 km in length. To demonstrate this, here we propagate 245-fs pulses over a 2.5-km DCF link made of the same SMF and DCF.

The 62-fs pulses [power spectrum shown in Fig. 3(a)] used in the previous experiments are spectrally tailored using an interference bandpass filter centered at 1560 nm to produce a filtered spectrum with a FWHM of ~9.8 nm as shown in Fig. 8, which would result in a transform-limited pulsewidth of 230 fs. The modulation of ~1.2 nm in the filtered spectrum is likely due to the Fabry–Perot effect associated with the interference filter. The filtered pulses were measured to have pulsewidths of 245 fs. Fig. 9(a) shows the cross-correlation trace of such filtered pulses with the original 62-fs pulses as the reference. These filtered 245-fs pulses with an average power of 50 μW at 33-MHz repetition rate are then sent to a 2.5-km SMF–DCF fiber link. The pulses initially broaden to ~400 ps (calculated) in 2060 m of SMF (AT&T 5D) and are then recompressed to ~500 fs FWHM using 445 m of DCF (AT&T JRFDC1074C1DC), resulting in a compression ratio of ~800. The cross-correlation traces of the input pulses and the optimally recompressed output pulses, measured using the original 62-fs laser pulses as the reference, are shown in Fig. 9(b). Note that because the path of the signal pulses (2.5 km of fiber) is much longer than that of the reference pulses (~2 m of free space), the $\#N$ output pulse is correlating with the $\#N + 387$ instead of the $\#N$ reference pulse. As in our previous 42-m experiments using shorter 62-fs pulses, the output pulse shown in Fig. 9(b) displays an oscillatory

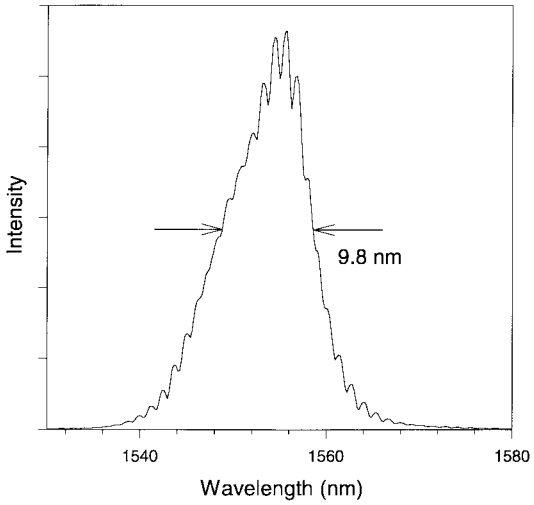

Fig. 8. Spectrum of the pulses after passing through the bandpass interference filter. The filtered spectrum corresponds to a bandwidth-limited pulsewidth of 230 fs. The modulation in the spectrum is likely due to the Fabry–Perot effect of the interference filter.

behavior in the trailing edge, indicating some uncompensated third-order dispersion (or dispersion slope). The spectral interferometry technique used to measure the previous 42-m link cannot be applied here to this 2.5-km SMF–DCF link because the timing jitter of the pulse source washes out the interference of the $\#N$ and $\#N + 387$ pulses. However, because our filtered pulses are substantially bandwidth-limited, by performing numerical simulations we estimate the residual third-order dispersion β_3 of our 2.5-km fiber link The result of our estimate is $\beta_3 \approx 0.023 \pm 0.007$ ps^3/km. This is roughly consistent with the residual dispersion in the previous 42-m link ($\sim$0.016 ps^3/km) [21] and also is $\sim$4 times lower than the dispersion slope of DSF. The observation the residual β_3 is somewhat worse than in the 42-m link case can probably be attributed to slight nonuniformities of the dispersions of the SMF and DCF along their lengths and, to a small extent, to the fact that the optimal length ratio is larger (4.63 versus 4.57) due to different center wavelength ($\sim$1560 nm versus $\sim$1591 nm). The transmission distance of 2.5 km should be suitable for local-area networking applications based on specially coded femtosecond light pulses [2]. Compared to previous experiments using sub-500-fs pulses and fiber gratings to compensate the dispersion of $\sim$250-m of single-mode fiber [3], our experiments achieve an $\sim 8\times$ longer propagation distance over SMF. It is also interesting to compare to the TDM systems experiments of Kawanishi *et al.* [17], in which 0.98-ps pulses were transmitted over 40 km with a broadening ratio of $\sim$1.6. Those experiments employed a dispersion-slope compensating fiber to reduce the overall dispersion slope D' from 0.06 to $\sim$0.02 ps/km/nm^2 (or $\beta_3 = 0.033$ ps^3/km). Our SMF–DCF link achieves a somewhat lower residual dispersion slope and should therefore allow even a longer transmission distance if the same 0.98-ps pulses are applied.

VI. Summary

We have demonstrated a dispersion compensation technique using a special DCF for femtosecond pulse transmission.

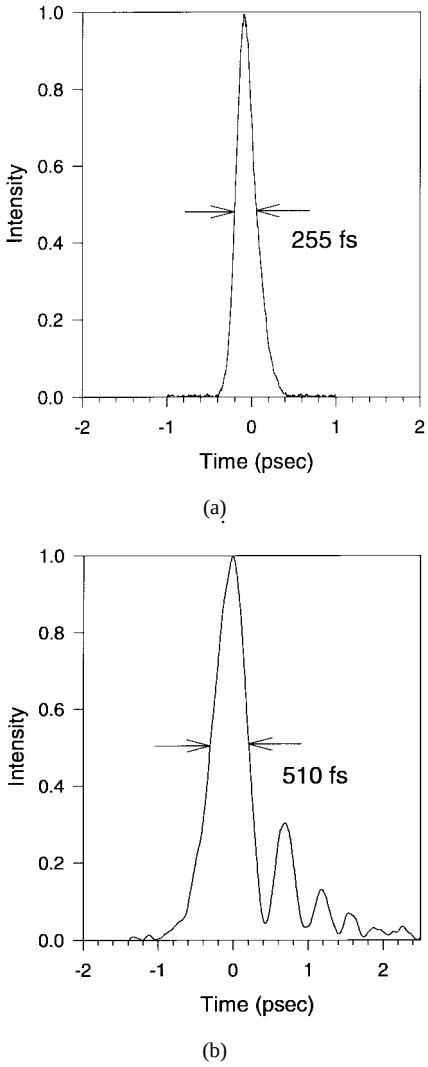

Fig. 9. 2.5-km fiber transmission for 245-fs pulses. Intensity profiles of (a) the input 245-fs pulse and (b) the output pulse of the 2.5-km optimally dispersion-compensated fiber link,measured by cross correlations using a 62-fs reference pulse directly from the lasers. 255 fs and 510 fs correspond, respectively, to $\sim$245 fs and $\sim$505 fs in pulse duration after deconvolution.

A short SMF–DCF link (42 m) was first tested using very short pulses (62 fs) to precisely test the dispersion compensation capability of this DCF. The residual dispersion of this dispersion-compensated link was then measured by using a femtosecond spectral interferometry technology. The results show that this optimized SMF–DCF link has a dispersion slope approximately six times lower than that of dispersion-shifted fiber. Finally, by performing experiments with 245-fs pulses over a 2.5-km SMF–DCF link, we have verified that the propagation distance scales as the cube of the pulsewidth, as expected for a link dominated by third-order dispersion. This length is already suitable for femtosecond local-area networking applications. Transmission of shorter femtosecond pulses over even longer distances may be accomplished by using appropriate pairs of dispersion compensating fibers, femtosecond pulses shapers [35], or other methods to further compensate for the residual third-order dispersion in our current compensated links.

ACKNOWLEDGMENT

The authors thank A. M. Vengsarkar and D. W. Peckham (Bell Laboratories) for the DCF and SMF fibers used in the dispersion compensation experiments. They also thank J. M. Wiesenfeld and P. J. Delfyett for their helpful discussions.

REFERENCES

[1] S. Kawanishi, H. Takara, O. Kamatani, and M. Saruwatari, "200 Gbit/s 100 km time-division-multiplexed optical transmission using supercontinuum pulses with prescaled PLL timing extraction and all-optical demultiplexing," *Electron. Lett.*, vol. 31, pp. 816–817, 1995.

[2] J. A. Salehi, A. M. Weiner, and J. P. Heritage, "Coherent ultrashort light pulse code-division multiple access communication systems," *J. Lightwave Technol.*, vol. 8, pp. 478–491, 1990.

[3] R. Kashyap, S. V. Chernikov, P. F. McKee, and J. R. Taylor, "30 ps chromatic dispersion compensation of 400 fs pulses at 100 Gbits/s in optical fibers using an all fiber photoinduced chirped reflection grating," *Electron. Lett.*, vol. 30, pp. 1078–1080, 1994.

[4] S. V. Chernikov, J. R. Taylor, and R. Kashyap, "Optical fiber dispersion compensation at 100 Gbits/s by using a novel transmission fiber based on chirped fiber Bragg gratings," in *Conf. Laser and Electo-optics*, Baltimore, MD, May 1995.

[5] B. J. Eggleton, F. Ouellette, K. A. Ahmed, P. A. Krug, and H.-F. Liu, "Recompression of pulses broadened by transmission through 10 km of nondispersion-shifted fiber at 1.55 μm using 40-mm-long optical fiber Bragg gratings with tunable chirp and central wavelength," *IEEE Photon. Technol. Lett.*, vol. 7, pp. 494–496, 1995.

[6] L. Dong, M. J. Cole, A. D. Ellis, M. Durkin, M. Ibsen, V. Gusmeroli, and R. I. Laming, "40 Gbit/s 1.55 μm transmission over 109 km of nondispersion shifted fiber with long continously chirped fiber gratings," in *Tech. Dig. Optical Fiber Communication Conf., OFC 97*, 1997, pp. 391–394, paper PD-6.

[7] M. Stern, J. P. Heritage, and E. W. Chase, "Grating compensation of third-order fiber dispersion," *IEEE J. Quantum Electron.*, vol. 28, pp. 2742–2748, 1992.

[8] S. Watanabe, T. Naito, and T. Chikama, "Compensation of chromatic dispersion in a single-mode fiber by optical phase conjugation," *IEEE Photon. Technol. Lett.*, vol. 5, pp. 92–95, 1993.

[9] R. M. Jopson, A. H. Gnauck, and R. M. Derosier, "10-Gb/s 360-km transmission over normal-dispersion fiber using mid-system spectral inversion," in *OFC 93*, San Jose, CA, 1993, pp. 17–20.

[10] A. D. Ellis, M. C. Tatham, D. A. O. Davies, D. Nessett, D. G. Moodie, and G. Sherlock, "40 Gbit/s transmission over 202 km of standard fiber using midspan spectral inversion," *Electron. Lett.*, vol. 31, pp. 299–301, 1995.

[11] A. H. Gnauck, R. M. Jopson, P. P. Iannone, and R. M. Derosier, "Transmission of two wavelength-multiplexed 10 Gbit/s channels over 560 km of dispersive fiber," *Electron. Lett.*, vol. 30, pp. 727–728, 1994.

[12] J. M. Dugan, A. J. Price, M. Ramadan, D. L. Wolf, E. F. Murphy, A. J. Antos, D. K. Smith, and D. W. Hall, "All-optical, fiber-based 1550 nm dispersion compensation in a 10 Gbit/s, 150 km transmission experiment over 1310 nm optimized fiber," in *Optical Fiber Communication*. Washington, DC: Opt. Soc. Amer., 1992, OSA Technical Digest Series, vol. 5, paper PD-14.

[13] H. Izadpanah, C. Lin, J. Gimlett, D. W. Hall, and D. K. Smith, "Dispersion compensation in 1310 nm-optimized SMF's using an equalizer fiber, EDFA's and 1310/1550 nm WDM," *Electron. Lett.*, vol. 28, pp. 1469–1471, 1992.

[14] A. J. Antos, D. W. Hall, and D. K. Smith, "Dispersion-compensating fiber for upgrading existing 1310-nm-optimized systems to 1550-nm operation," in *Tech. Dig. Optical Fiber Communication Conf., OFC 93*, 1993, pp. 204–205, paper THJ3.

[15] C. D. Poole, J. M. Wiesenfeld, D. J. DiGiovanni, and A. M. Vengsarkar, "Optical fiber-based dispersion compensation using high-order modes near cut-off," *J. Lightwave Technol.*, vol. 12, pp. 1746–1758, 1994.

[16] C.-C. Chang and A. M. Weiner, "Dispersion compensation for ultrashort pulse transmission using two-mode equalizer fibers," *IEEE Photon. Technol. Lett.*, vol. 6, pp. 1392–1394, 1994.

[17] S. Kawanishi, H. Takara, T. Morioka, O. Kamatani, K. Kikoh, and M. Saruwatari, "Single channel 400 Gbit/s time-division-multiplexed transmission of 0.98 ps pulses over 40 km employing dispersion slope compensation," *Electron. Lett.*, vol. 9, pp. 457–459, 1996.

[18] J. P. Gordon, "Theory of the soliton self-frequency shift," *Opt. Lett.*, vol. 11, pp. 662–664, 1986.

[19] C. Lin, H. Kogelnik, and L. G. Cohen, "Optical-pulse equalization of low-dispersion transmission in single-mode fibers in the 1.3–1.7 μm spectral region," *Opt. Lett.*, vol. 5, pp. 476–478, 1980.

[20] A. M. Vengsarkar, A. E. Miller, M. Haner, A. H. Gnauck, W. A. Reed, and K. L. Walker, "Fundamental-mode dispersion-compensating fibers: Design consideration and experiments," in *OFC Tech. Dig.*, 1994, pp. 225–227, paper Thk2.

[21] C.-C. Chang, A. M. Weiner, A. M. Vengsarkar, and D. W. Peckham, "Broadband fiber dispersion compensation for sub-100-fs pulses with a compression ratio of 300," *Opt. Lett.*, vol. 21, pp. 1141–1143, 1996.

[22] K. Tamura, E. P. Ippen, H. A. Haus, and L. E. Nelson, "77-fs pulse generation from a stretched-pulse mode-locked all-fiber ring laser," *Opt. Lett.*, vol. 18, pp. 1080–1082, 1993.

[23] W. J. Tomlinson, R. H. Stolen, and A. M. Johnson, "Optical wave breaking of pulses in nonlinear optical fibers," *Opt. Lett.*, vol. 10, pp. 457–459, 1985.

[24] L. G. Cohen, "Comparison of single-mode fiber dispersion measurement techniques," *J. Lightwave Technol.*, vol. 3, pp. 958–966, 1985.

[25] W. H. Knox, "Dispersion measurements for femtosecond-pulse generation and applications," *Appl. Phys. B*, vol. 58, pp. 225–235, 1994.

[26] H.-T. Shang, "Chromatic dispersion measurement by white-light interferometry on meter-length single-mode optical fibers," *Electron. Lett.*, vol. 17, pp. 603–605, 1981.

[27] J. Stone and D. Marcuse, "Direct measurement of second-order dispersion in short optical fibers using white-light interferometry," *Electron. Lett.*, vol. 20, pp. 751–752, 1984.

[28] F. Reynaud, F. Salin, and A. Barthelemy, "Measurement of phase shifts introduced by nonlinear optical phenomena on subpicosecond pulses," *Opt. Lett.*, vol. 14, pp. 275–277, 1989.

[29] X. D. Cao and D. D. Meyerhofer, "Frequency-domain interferometer for measurement of the polarization mode dispersion in single-mode optical fiber," *Opt. Lett.*, vol. 19, pp. 1837–1839, 1994.

[30] L. Lepetit, G. Cheriaux, and M. Joffre, "Linear techniques of phase measurement by femtosecond spectral interferometry for application in spectroscopy," *J. Opt. Soc. Amer. B*, vol. 12, pp. 2467–2474, 1995.

[31] V. Binjrajka and A. M. Weiner, "Effect of self-phase modulation on ultrashort pulse transmission in dispersion compensated systems with large broadening and compression," in *CLEO'96 Tech. Dig.*, 1996, pp. 397–398, paper CThk8.

[32] C. X. Yu, S. Namiki, W. S. Wong, and H. A. Haus, "Noise performance of the stretched-pulse ring laser," in *CLEO '96*, 1996, paper CFD6.

[33] P. J. Delfyett, L. T. Florez, N. Stoffel, T. Gmitter, N. C. Andreadakis, Y. Siberberg, J. P. Heritage, and G. A. Alphonse, "High-power ultrafast laser diodes," *IEEE J. Quantum Electron.*, vol. 28, pp. 2203–2219, 1992.

[34] G. P. Agrawal, *Nonlinear Fiber Optics*, 2nd ed. San Diego, CA: Academic, 1995, ch. 11.

[35] A. M. Weiner, D. E. Leaird, J. S. Patel, and J. R. Wullert, II, "Programmable shaping of femtosecond optical pulses by use of 128-element liquid crystal phase modulator," *IEEE J. Quantum Electron.*, vol. 28, pp. 908–920, 1992.

Cheng-Chun Chang was born in Taipei, Taiwan, in 1963. He received the B.S. degree in civil engineering from National Taiwan University in 1985, the M.S. degrees in engineering science and mechanics and electrical engineering from Virginia Polytechnic Institute and State University, Blacksburg, in 1990 and 1992, respectively. He is currently pursuing the Ph.D. degree in electrical engineering at Purdue University, West Lafayette, IN. His research is involved with ultrashort pulse fiber lasers, fiber dispersion compensation, femtosecond pulse-shaping, and femtosecond code-division multiple access (CDMA) systems.

He served in the Army of the Republic of China from 1985 to 1987.

Andrew M. Weiner (S'84–M'84–SM'91–F'95) was born in Boston, MA, in 1958. He received the Sc.D. degree in electrical engineering from the Massachusetts Institute of Technology (MIT), Cambridge, in 1984. His doctoral dissertation dealt with femtosecond pulse compression (including generation of the shortest optical pulses reported up to that time) and measurement of femtosecond dephasing in condensed matter.

From 1979 through 1984, he was a Fannie and John Hertz Foundation Graduate Fellow at MIT. In 1984, he joined Bellcore where he conducted research on ultrafast optics, including shaping of ultrashort pulses, nonlinear optics and switching in fibers, and spectral holography. In 1989 he became Manager of the Ultrafast Optics and Optical Signal Processing Research District. He assumed his current position as Professor of Electrical and Computer Engineering at Purdue University, West Lafayette, IN, in October 1992. Since August 1996, he has also been serving as Director of Graduate Admissions for the School of Electrical and Computer Engineering. His current research interests center on holography of ultrashort pulses, high-speed optical communications, applications of pulse shaping to femtosecond spectroscopy and nonlinear optics, and optical imaging in scattering media. He is currently Topical Editor of *Optics Letters* and previously served as Associate Editor of IEEE JOURNAL OF QUANTUM ELECTRONICS and IEEE PHOTONICS TECHNOLOGY LETTERS. He has also served as vice-chairman of the Gordon Conference on Nonlinear Optics and Lasers, chair of the Ultrafast Phenomena Technical Group of the Optical Society of America (OSA), chair of the OSA Lomb Medal Committee, member of the IEEE Education Medal Committee and of the IEEE Quantum Electronics Award Committee, and member of numerous conference committees. He was Program Co-Chair for the 1996 Conference on Laser and Electro-optics. In 1988–1989, he served as IEEE Lasers and Electro-optics Society (LEOS) Traveling Lecturer. He has authored approximately 170 conference and university talks and approximately 100 technical articles, including four book chapters, and is holder of five U.S. patents.

Dr. Weiner is a fellow of the OSA and a member of the IEEE LEOS Board of Governors. He was awarded the 1984 Hertz Foundation Doctoral Thesis Prize, and in 1990, he was awarded the Adolph Lomb Medal of the OSA for noteworthy contributions to optics made before reaching the age of 30. He is also a recipient of the 1997 ASEE Curtis W. McGraw Research Award.